

# Introducing dual excitation and tunable dual emission in ZnO through selective lanthanide (Er<sup>3+</sup>/Ho<sup>3+</sup>) doping

Cite this: *RSC Adv.*, 2014, 4, 18811

Naveen Khichar, Swati Bishnoi and Santa Chawla\*

We have introduced dual excitation properties in the multifunctional semiconductor ZnO by controlled solid state diffusion of dopant lanthanide ions like Er<sup>3+</sup> and Ho<sup>3+</sup> into the lattice at 500 °C. So far light emission from doped ZnO has been explored either under UV or IR excitation. Our results show that the emission colour can be tuned from cyan to red under UV (band edge, 377 nm) excitation and from green to red under IR (980 nm) excitation in ZnO through selected doping of lanthanide ions. Doping lanthanide ions in ZnO changes its morphology and emission characteristics. Whereas down conversion emission under UV excitation is due to across band gap excitation and subsequent donor–acceptor pair recombination, the dependence of up conversion emission yield on pump laser power indicates that two to three photon processes may be more effective in ZnO hosts for frequency upconversion.

Received 12th February 2014  
Accepted 10th April 2014

DOI: 10.1039/c4ra01248h

[www.rsc.org/advances](http://www.rsc.org/advances)

## 1. Introduction

Rare-earth (RE) ion doped nanomaterials with up-conversion (UC) luminescence have a variety of applications in solid-state lasers, three dimensional displays, solar cells and fluorescence biological labels and have attracted a great deal of attention.<sup>1–4</sup> Most such materials comprise complex inorganic hosts of insulators, mainly fluorides. Efficient light emitting properties from RE ions doped in semiconductor nanoparticles has been a challenge. The ZnO crystal, a direct band-gap multifunctional semiconductor with excellent physical and chemical stability has been identified as an efficient light emitter and has received extensive attention in the field of photonic technology.<sup>5–15</sup> RE ion doped ZnO have also applications in high power lasers and various optoelectronic devices.<sup>16,17</sup> Luminescence studies in ZnO mostly focused on Stokes shifted emission under UV excitation. Reports on anti Stokes UC luminescence in ZnO are sparse *e.g.*, in ZnO:Er<sup>3+</sup> and Er<sup>3+</sup>, Yb<sup>3+</sup> codoped ZnO<sup>18–21</sup> and in Ho<sup>3+</sup> and Yb<sup>3+</sup> co-doped ZnO.<sup>22</sup> In most UC studies, Yb<sup>3+</sup> ion is used as sensitizer for efficient IR absorption and energy transfer processes to RE ion. However, tunability in Stokes shifted luminescence characteristics of ZnO due to doping of Er<sup>3+</sup> and Ho<sup>3+</sup> under UV excitation has not been investigated.

In this work, we provide the first report on dual excitation and dual emission characteristics of RE ion doped ZnO which are excitable by both UV and IR light but exhibit different emission colour depending upon the dopant. ZnO with different rare earth ion doping *e.g.*, ZnO, ZnO:Er<sup>3+</sup>, ZnO:Er<sup>3+</sup>, Yb<sup>3+</sup>, ZnO:Ho<sup>3+</sup>, ZnO:Ho<sup>3+</sup>, Yb<sup>3+</sup> were synthesized by controlled

solid state diffusion at relatively low temperature (500 °C). A detail photoluminescence (PL) spectroscopic study of RE doped ZnO under both UV and IR (980 nm) excitation clearly indicate that they exhibit dual mode luminescence characteristics.

## 2. Experimental

For preparation of undoped ZnO; ZnO:Er<sup>3+</sup> (2 mol%); ZnO:Er<sup>3+</sup> (2 mol%), Li (2%); ZnO:Er<sup>3+</sup> (2 mol%), Yb<sup>3+</sup> (10 mol%); ZnO:Ho<sup>3+</sup> (2 mol%) and ZnO:Ho<sup>3+</sup> (2 mol%), Yb<sup>3+</sup> (10 mol%) by controlled reaction in the solid state, stoichiometric molar compositions of commercial ZnO powder and dopant lanthanide oxide materials Er<sub>2</sub>O<sub>3</sub>, Ho<sub>2</sub>O<sub>3</sub>, Yb<sub>2</sub>O<sub>3</sub> and LiOH·2H<sub>2</sub>O were taken according to stoichiometric formula with lanthanide ions as substitutional dopant in zinc position. All the powder precursors were mixed thoroughly in pestle–mortar and then packed in highly pure quartz boat. The material was fired at 500 °C for 2 hours in air atmosphere. The sintered white mass was allowed to cool naturally as slow cooling rate allows uniform temperature distribution throughout the reacting mixture enabling better dopant substitution and luminescence intensity in the product. Finally a white sintered mass is obtained after cooling which is made into powder form by grinding.

## 3. Characterisation

The X-ray powder diffraction (XRD) of the synthesized samples was examined on a Rigaku miniflex X-ray diffractometer using the principle of Bragg–Brentano geometry, with Cu-K $\alpha$  radiation (1.54 Å). Diffractograms were recorded in grazing incidence geometry. The diffraction angle 2 $\theta$  was scanned in the range 20 to 80°.

Luminescent Materials Group, CSIR-National Physical Laboratory, Dr. K. S. Krishnan Road, New Delhi – 110012, India. E-mail: [santa@nplindia.org](mailto:santa@nplindia.org)

The morphology of the synthesized undoped and Lanthanide doped ZnO powder samples were inspected using a LEO 440 PC based digital scanning electron microscope (SEM).

The photoluminescence (PL) down and up conversion properties like excitation, emission spectra and time resolved decay of luminescence were recorded using combined steady state fluorescence and lifetime spectrometer of Edinburgh Instruments FLSP920 with Xe lamp as excitation source for down conversion experiments. For up conversion photoluminescence measurements, a power tunable 980 nm diode laser (MDL-N-980-6W) coupled with optical fibre, was used as excitation source. For measurements of time resolved luminescence decay under UV excitation, microsecond pulsed Xe lamp was used and time correlated single photon counting (TCSPC) technique was used.

## 4. Results and discussion

### 4.1 Phase characterization

Phase characterization of all synthesized undoped and lanthanide doped ZnO samples was done by X-ray diffraction and Fig. 1 shows the intensities of main three peaks (100), (002) and (101) corresponding to “wurtzite hexagonal” phase of ZnO (JCPDS Card no. 36-1451). All the peaks of ZnO; ZnO:Er<sup>3+</sup>; ZnO:Ho<sup>3+</sup>; ZnO:Ho<sup>3+</sup>, Yb<sup>3+</sup>; ZnO:Er<sup>3+</sup>, Li<sup>+</sup> synthesized by SSR method are monophasic and could be indexed to “wurtzite hexagonal” phase of ZnO without any precipitated phase. The sharp peaks of ZnO indicate that the products are well crystallized and that Er<sup>3+</sup>, Yb<sup>3+</sup>, Ho<sup>3+</sup> and Li<sup>+</sup> doping in ZnO does not alter its wurtzite structure. The changes in peak intensities due to Er<sup>3+</sup>, Yb<sup>3+</sup>, Ho<sup>3+</sup> and Li<sup>+</sup> doping indicate that due to doping diffracted peak intensity decreases. A close comparison of the diffraction angle with different doping (Fig. 1) suggests peak shift and hence change in lattices parameters due to substitutional doping of Er<sup>3+</sup> (effective ionic radii 0.103 nm), Yb<sup>3+</sup> (effective ionic radii 0.101 nm), Ho<sup>3+</sup> (effective ionic radii

0.104 nm), in place of Zn<sup>2+</sup> (effective ionic radii 0.088 nm). The powder X-ray diffraction spectra of ZnO:Er<sup>3+</sup>, Yb<sup>3+</sup> sample shows poor crystallinity compared to other samples as well as presence of peaks other than ZnO occurring from RE precursors (inset of Fig. 1). The variation of lattice parameters ‘a’ and ‘c’ with doping of Er<sup>3+</sup>, Yb<sup>3+</sup>, Ho<sup>3+</sup> and Li<sup>+</sup> in ZnO is shown in Table 1. As substitutional Er<sup>3+</sup> has larger ionic radius (0.103 nm) than Zn<sup>2+</sup> (0.088 nm), Er–O bond contraction would result in decrease in crystalline parameters ‘a’ and ‘c’ as evidenced in Table 1. Charge compensation by addition of monovalent Li<sup>+</sup>, however restores the lattice parameters of undoped ZnO.

### 4.2 Morphology

The SEM micrographs of ZnO with different rare earth doping are shown in Fig. 2. The pure undoped ZnO sample consist of rounded grains that sometimes coalesce to form a floral morphology, while all the doped ZnO sample exhibit flake like morphology as shown in Fig. 2. As all the samples have been prepared under identical synthesis condition, the change in morphology could only be due to strain induced in the lattice by doping larger RE ions. Dopant induced morphology changes in ZnO have also been reported earlier.<sup>23,24</sup>

### 4.3 Down conversion luminescence

The photoluminescence excitation and emission spectra (Fig. 3) and corresponding photographs of powder samples under UV (377 nm) excitation displayed as insets clearly reveal the tunable emission from ZnO due to doping of rare earth ions. The excitation spectra shows sharp band edge absorption of ZnO at 377 nm for all undoped as well as doped samples and all PL emission spectra are recorded under 377 nm excitation. Undoped ZnO shows broad blue green (cyan) emission peaking at 505 nm. The intrinsic cyan luminescence of undoped ZnO changes due to lanthanum doping and ZnO:Er<sup>3+</sup> sample emits broad red emission peaking at 626 nm and Ho<sup>3+</sup> doped ZnO sample emits broad red emission peaking at 619 nm. With addition of co dopant Yb<sup>3+</sup>, the ZnO:Ho<sup>3+</sup>, Yb<sup>3+</sup> sample also emits in red region with broad emission maxima at 625 nm. The emission under UV excitation originates due to donor–acceptor pair (DAP) recombination between various intrinsic and extrinsic (dopant related) defects. As the trap level energy position

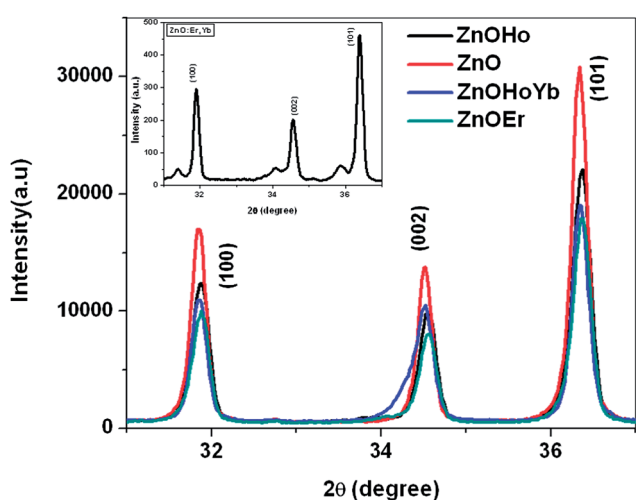


Fig. 1 Comparison between XRD patterns of undoped ZnO and ZnO with different rare earth doping, inset shows the XRD spectra of ZnO:Er, Yb.

Table 1 Change in lattice parameters and luminescence decay time due to lanthanide doping in ZnO

Sample	Crystallite parameter		Luminescence decay time $\tau$ (microsecond) (relative%)	
	<i>a</i>	<i>c</i>	$\tau_1$	$\tau_2$
Undoped ZnO	3.2407	5.1922	1.35 (30.45%)	8.47 (69.55%)
ZnO:Er <sup>3+</sup>	3.2387	5.1864	3.51 (24.09%)	23.68 (75.97%)
ZnO:Er <sup>3+</sup> , Li	3.2407	5.1922	—	—
ZnO:Er <sup>3+</sup> , Yb <sup>3+</sup>	3.2469	5.1907	1.636 (31.65%)	20.58 (68.35%)
ZnO:Ho <sup>3+</sup>	3.2387	5.1864	3.38 (20.54%)	27.5 (79.46%)
ZnO:Ho <sup>3+</sup> , Yb <sup>3+</sup>	3.2407	5.1922	1.60 (36.86%)	23.24 (63.14%)

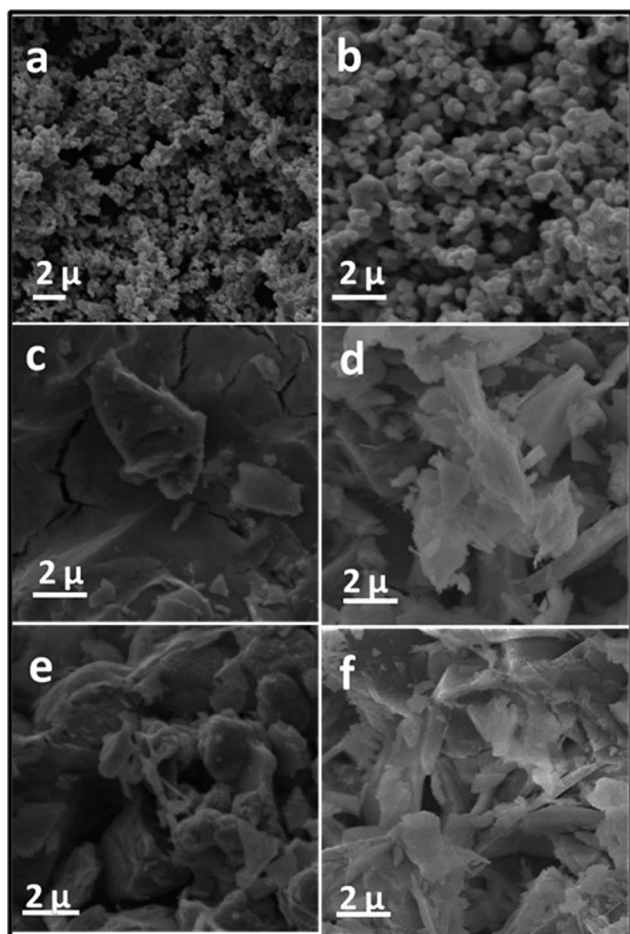
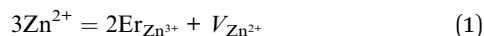


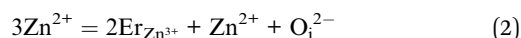
Fig. 2 SEM image of (a) ZnO (b) ZnO annealed (c) Er<sup>3+</sup> doped ZnO (d) Er<sup>3+</sup>:Yb<sup>3+</sup> doped ZnO (e) Ho<sup>3+</sup> doped ZnO (f) Ho<sup>3+</sup>:Yb<sup>3+</sup> doped ZnO.

changes due to different donor levels corresponding to Er<sup>3+</sup>, Yb<sup>3+</sup> and Ho<sup>3+</sup>, the broad peak due to DAP recombination shifts.

Charge compensation in ZnO doped with Er<sup>3+</sup>/Ho<sup>3+</sup> and Yb<sup>3+</sup> would require that *e.g.*, two Er<sup>3+</sup> ions are substituted for three Zn<sup>2+</sup> ions. For trivalent state of Er<sup>3+</sup> dopant, overall charge neutrality in the lattice could be maintained either by creating one Zn<sup>2+</sup> vacancy for incorporation of each two Er<sup>3+</sup> ions or introducing one oxygen interstitial (O<sub>i</sub><sup>2-</sup>) defect in the following manner:



or,



Both the point defects  $V_{\text{Zn}}$  (0.3 eV above valence band) and  $\text{O}_i$  (1.08 eV above the valence band) act as acceptor centres in ZnO,<sup>25</sup> but formation probability of interstitial oxygen centres ( $\text{O}_i$ ) is less due to bigger size of oxygen atoms (0.126 nm). On the contrary, as the ZnO samples are synthesized in oxygen rich atmosphere, zinc vacancies are more favourable as they have very low formation energy.  $V_{\text{Zn}}$  centre lies 0.3 eV above ZnO valence band.<sup>25</sup> Recombination of electrons from an intrinsic

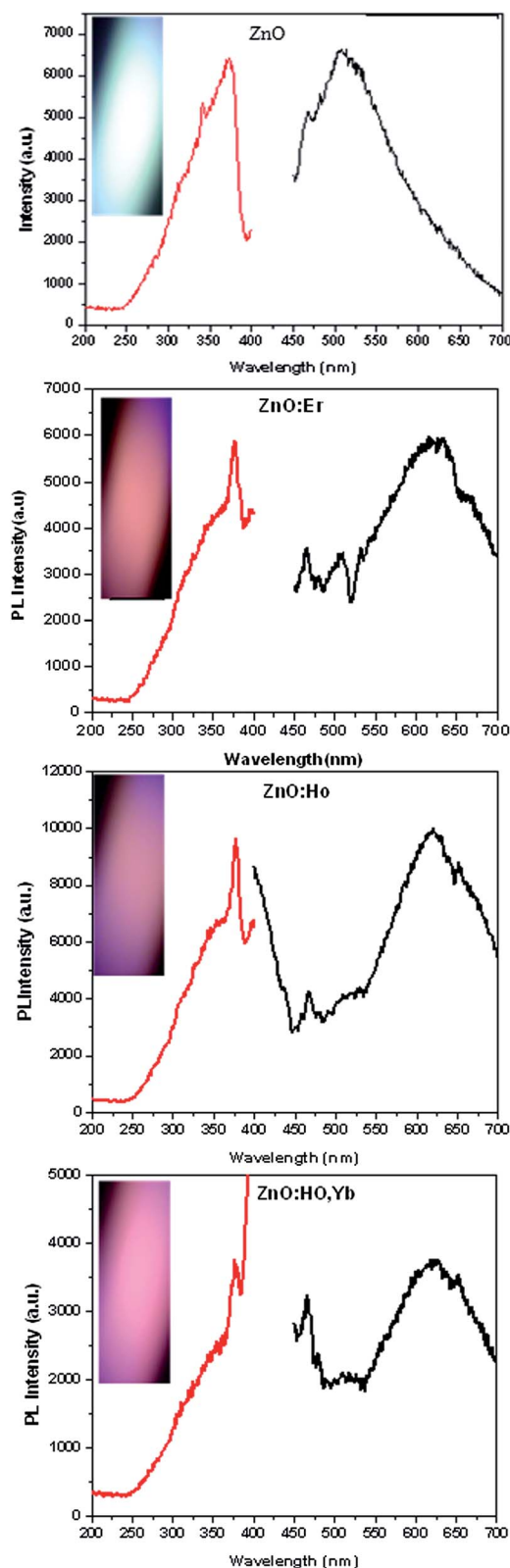


Fig. 3 Downconversion emission spectra under UV excitation of undoped and various lanthanide doped ZnO samples. The inset shows the photograph of the samples under UV light.

donor level to  $V_{\text{Zn}}$  acceptor centre give rise to blue green (cyan) emission in undoped ZnO (Fig. 3, inset). On doping  $\text{Er}^{3+}/\text{Ho}^{3+}$  in ZnO, the intrinsic point defects created by trivalent dopants in zinc substitutional position makes donor centres and also enhances the presence of zinc vacancies in the neighbourhood for charge compensation. Recombination between such donor-acceptor pair give rise to red luminescence in  $\text{Er}^{3+}/\text{Ho}^{3+}$  doped ZnO. The excitation and recombination processes are elucidated in the energy level diagram (Fig. 5).

#### 4.4 Up conversion luminescence

The upconversion photoluminescence emission spectra of rare earth ion doped ZnO samples under different excitation laser (980 nm) power are shown in Fig. 4. The UC spectra of  $\text{ZnO}:\text{Er}^{3+}$  sample exhibit dominant red emission (peak at 663 nm) corresponding to transition from level  $4\text{F}_{9/2}-4\text{I}_{15/2}$  and smaller green emission peaks (at 523 nm and 545 nm). The  $\text{ZnO}:\text{Er}^{3+}, \text{Yb}^{3+}$  sample shows change in the ratio of red and green emission.  $\text{ZnO}:\text{Er}^{3+}, \text{Li}^{+}$  samples show very poor UC emission.  $\text{ZnO}:\text{Ho}^{3+}$  sample emits green (peak at 545 nm) and red (peak at 652 nm) in comparable proportion resulting in a green yellow fluorescent colour.  $\text{ZnO}:\text{Ho}^{3+}, \text{Yb}^{3+}$  sample shows predominantly green peak at 545 nm yielding green UC fluorescence and

about 70 times increase in green UC luminescence is observed due to  $\text{Yb}^{3+}$  codoping. Though in most UC phosphors, UC emission intensity increases with  $\text{Yb}^{3+}$  codoping, in case of  $\text{ZnO}:\text{Er}^{3+}, \text{Yb}^{3+}$  the UC emission intensity decreased. This has happened due to poor crystallinity of  $\text{ZnO}:\text{Er}^{3+}, \text{Yb}^{3+}$  samples synthesized at 500 °C (shown as inset of Fig. 1) with presence of some unreacted precursors. Due to lattice strain arising from  $\text{Yb}^{3+}$  codoping in  $\text{ZnO}:\text{Er}^{3+}$ , 'a' and 'c' value change to 3.2469 Å and 5.1907 Å compared to that of undoped ZnO – 3.2407 Å and 5.1922 Å (Table 1). Whereas  $\text{ZnO}:\text{Ho}^{3+}, \text{Yb}^{3+}$  samples show very good crystallinity with lattice parameters corresponding well with that of undoped ZnO. Due to this, the PL emission both under UV and IR excitation from  $\text{ZnO}:\text{Er}^{3+}, \text{Yb}^{3+}$  samples are very poor. Moreover, it has also been reported that higher  $\text{Yb}^{3+}$  concentration that 5 mol% in  $\text{ZnO}:\text{Er}^{3+}, \text{Yb}^{3+}$  lead to decrease in intensity.<sup>21</sup>

As up conversion emission involves absorption of multiple photons of lower energy (IR) by the phosphor material to emit a single photon of higher energy (visible), the dependence of UC emission intensity ( $I_{\text{UC}}$ ) on the pump IR laser power ( $I_i$ ) follows a power law represented by  $I_{\text{UC}} \propto I_i^n$ . The upconversion emission efficiency is also dependent upon the non radiative multiphonon relaxation processes that are dependent upon the host

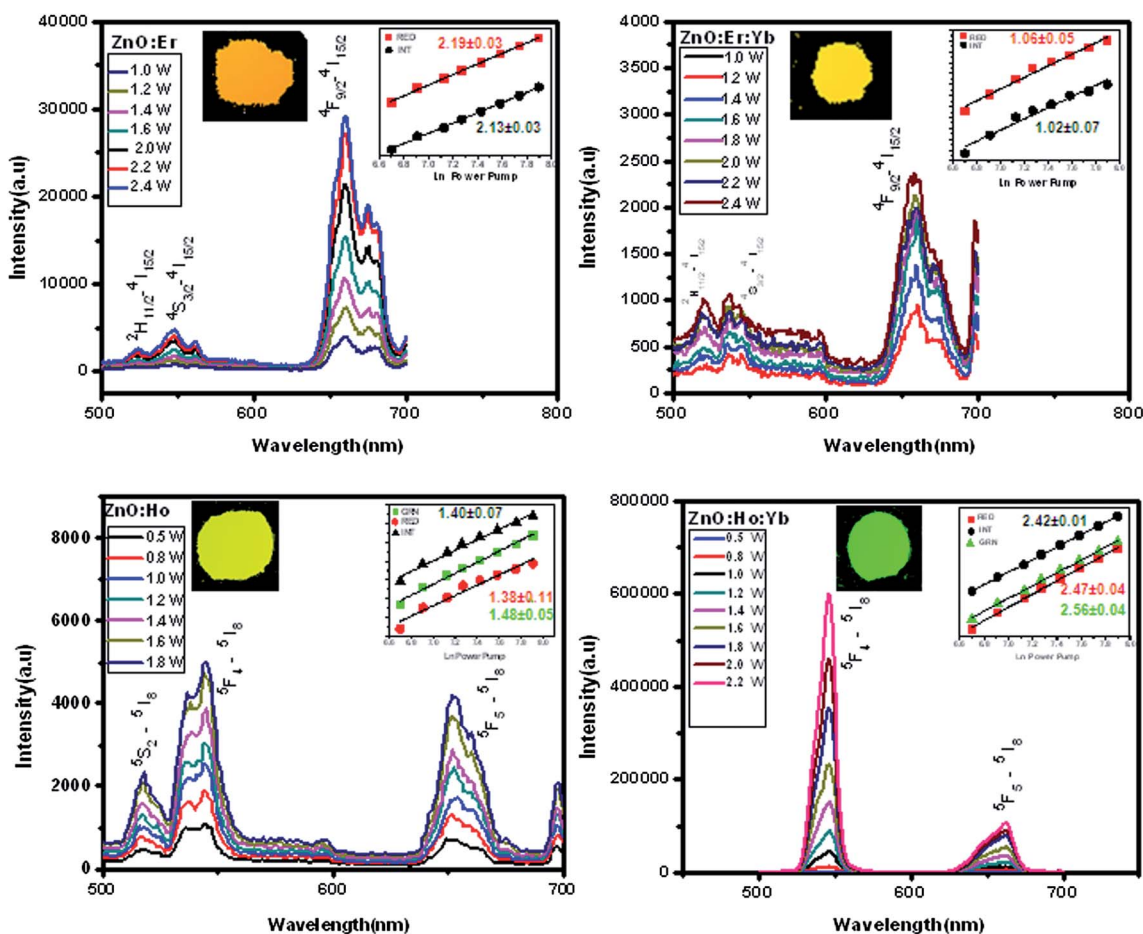


Fig. 4 Up conversion PL spectra and inset showing dependence of UC intensity with pump power of the green, red and integrated emission of ZnO doped with  $\text{Er}^{3+}$ ;  $\text{Er}^{3+}, \text{Yb}^{3+}$ ;  $\text{Ho}^{3+}$ ;  $\text{Ho}^{3+}, \text{Yb}^{3+}$ . The insets show the colour of samples under IR excitation.

lattice. The oxide semiconductor has low phonon energy with a characteristic  $440\text{ cm}^{-1}$  energy corresponding to Zn–O vibrational bond.<sup>19</sup> Low phonon energy of the host facilitates the active lanthanide ions to relax to ground state by emitting photons rather than phonons. In order to investigate the multiple photon absorption process in RE ion doped ZnO, the dependence of integrated up-converted emission intensity on IR laser excitation power has been calculated for each sample and is shown as the power pump plot in insets of each UC PL spectra. We have integrated the emission spectra separately under green emission region as well as red emission region and also the total integrated intensity of emission spectra and plotted against the pump laser power.

ZnO:Er<sup>3+</sup> samples displays slope of  $2.19 \pm 0.03$  for integrated emission and  $2.12 \pm 0.02$  for only red emission. For the ZnO:Er<sup>3+</sup>, Yb<sup>3+</sup> sample, the integrated emission slope value is 1.26 and red emission slope is 1.24. Similarly for ZnO:Ho<sup>3+</sup> sample, the slope values are  $1.38 \pm 0.11$ ,  $1.48 \pm 0.05$ ,  $1.40 \pm 0.07$  for red, green and integrated emission respectively. For ZnO:Ho<sup>3+</sup>, Yb<sup>3+</sup> sample, slope values are  $2.47 \pm 0.04$ ,  $2.56 \pm 0.04$ ,  $2.42 \pm 0.01$  for red, green and integrated emission respectively. The results indicate that two photon processes are mainly responsible for the observed up-converted emissions in Er<sup>3+</sup>/Ho<sup>3+</sup> doped ZnO. It is also evident for ZnO:Ho<sup>3+</sup>, Yb<sup>3+</sup> samples, the photon yield is very high and slope value is more than 2 suggesting that three photon absorption may be more effective for frequency upconversion process in ZnO host. The UC excitation process from ground state of the RE ion to respective emitting level may involve two to three photons depending upon the concentration of rare earth ions and possible energy transfer and cross relaxation processes between levels. Three photon processes have also been reported for ZnO:Er<sup>3+</sup>, Yb<sup>3+</sup> due to cross relaxation between levels<sup>21</sup> and in Y<sub>2</sub>O<sub>3</sub>:Er<sup>3+</sup>, Yb<sup>3+</sup>,<sup>26</sup> in ZrO<sub>2</sub>:Er<sup>3+</sup>,<sup>27</sup> in NaYF<sub>4</sub>:Er<sup>3+</sup>, Yb<sup>3+</sup>.<sup>28</sup>

#### 4.5 Energy level diagram

The excitation and emission processes for both down and up conversion luminescence are elucidated in the energy level diagram including the f–f levels of Er<sup>3+</sup>, Yb<sup>3+</sup>, Ho<sup>3+</sup> ions in Fig. 5. Under 377 nm band edge excitation, electrons excited to the conduction band can relax to various donor levels (intrinsic as well as created by dopant trivalent RE ion) and radiatively recombine with the acceptor centre to produce luminescence as indicated in Fig. 5.

Under 980 nm excitation, the emitter Er<sup>3+</sup> and Ho<sup>3+</sup> ions can directly get excited from their respective ground states to excited state *e.g.*,  $^4I_{15/2}$ – $^4I_{11/2}$  (Er<sup>3+</sup>) and  $^5I_8$ – $^5I_5$  (Ho<sup>3+</sup>) and then to upper levels by two photon absorption process as the respective level spacing correspond to excitation energy. In UC phosphors, usually Yb<sup>3+</sup> is codoped as a sensitizer since Yb<sup>3+</sup> ions can resonantly absorb 980 nm photons corresponding to the level spacing  $^2F_{7/2}$  to  $^2F_{5/2}$  and have larger excitation cross section than the emitter such as Er<sup>3+</sup> and Ho<sup>3+</sup>. Yb<sup>3+</sup> concentration is usually kept higher to ensure more number of Yb<sup>3+</sup> ions on the  $^2F_{5/2}$  excited state. Upon irradiation by 980 nm laser, two Yb<sup>3+</sup> ions resonantly absorb two IR photons and reach  $^2F_{5/2}$  excited

state when one Yb<sup>3+</sup> ion transfers energy to the second Yb<sup>3+</sup> ion (Fig. 5) to go back to ground state  $^2F_{7/2}$ . The excited Yb<sup>3+</sup> ion non-radiatively transfers the energy to neighbouring Ho<sup>3+</sup> ions exciting them to various upper levels from their respective ground state. Er<sup>3+</sup> and Ho<sup>3+</sup> ions emitting multiband light with Yb<sup>3+</sup> acting as a sensitizer has been reported in many papers.<sup>29–31</sup> The upconversion emission in Er<sup>3+</sup> are explained by several mechanisms such as<sup>19</sup> (a) Excited State Absorption (ESA) (b) Energy Transfer (ET) (c) Photon Avalanche (PA). In the present case, since no power threshold was observed, PA mechanism can be ruled out. For Yb<sup>3+</sup> sensitized samples, the excited Yb<sup>3+</sup> ion transfer its energy to Er<sup>3+</sup> ions, Er<sup>3+</sup> then undergoes  $^4I_{15/2}$ – $^4I_{11/2}$  and  $^4I_{11/2}$ – $^4F_{7/2}$  transition. Due to non-radiative process involving lattice phonons in Er<sup>3+</sup> the electron in the  $^4F_{7/2}$  state undergo nonradiative decay to  $^2H_{11/2}$ ,  $^4S_{3/2}$  and  $^4F_{9/2}$  level.<sup>20</sup> Finally in emission process the excited electrons in  $^4S_{3/2}$ ,  $^4F_{9/2}$ ,  $^2H_{11/2}$  transit back to  $^4I_{15/2}$  ground state giving rise to Er<sup>3+</sup> emission peaks at 525 nm, 545 nm and 663 nm. For only Er<sup>3+</sup> doped ZnO, since the red emission is dominant, the population of  $^4F_{9/2}$  level is high which could happen through ground state absorption from  $^4I_{15/2}$  level, excited state absorption from  $^4I_{11/2}$  and some cross relaxation between  $^4F_{7/2}$  and  $^4I_{11/2}$  levels as this provides a low energy loss ( $80\text{ cm}^{-1}$ ) pathway<sup>18</sup> compared to multiphonon relaxation from  $^4F_{7/2}$  level as the energy gap is high.

In Yb<sup>3+</sup>, Ho<sup>3+</sup> system, excited sensitizer ion Yb<sup>3+</sup> transfer energy to Ho<sup>3+</sup> ion exciting them to higher levels. Two consecutive ET from Yb<sup>3+</sup> to Ho<sup>3+</sup> can raise the Ho<sup>3+</sup> ions to the  $^5S_2$ ,  $^5F_4$  levels and the green emission occurs when Ho<sup>3+</sup> ions in the  $^5S_2$ ,  $^5F_4$  levels relax to ground state  $^5I_8$  by emission of green photons (Fig. 5). ESA from Ho<sup>3+</sup>  $^5I_6$ – $^5S_2$  can also raise the emitting Ho<sup>3+</sup> ions to the green emitting level as the pump laser energy matches well with the level spacing. Due to large population in  $^5S_2$ ,  $^5F_4$  levels, the green emission intensity is high. The non radiative relaxation probability from  $^5S_2$ ,  $^5F_4$  level to lower  $^5F_5$  level depends upon the host phonon energy and the red emission at 652 nm happens due to  $^5F_5$ – $^5I_8$  transition. The non radiative transition to  $^5F_5$  level reduces drastically upon codoping Yb<sup>3+</sup> ions and the green emission becomes very dominant with much higher emission intensity. The red emitting  $^5F_5$  level may be populated by  $^5I_7$ – $^5F_5$  absorption,<sup>32</sup> cross relaxation (CR) may also happen due to ion–ion interaction. From the slope of pump power plot, the UC process in ZnO:Ho<sup>3+</sup> (slope  $\sim 1.5$ ) is a two photon process whereas in ZnO:Ho<sup>3+</sup>, Yb<sup>3+</sup> (slope  $\sim 2.5$ ) is two to three photon process for excitation to  $^5S_2$ ,  $^5F_4$  levels and predominant green emission.

The UC and DC spectra described above clearly indicate that rare earth metal ions Er<sup>3+</sup>/Ho<sup>3+</sup> doped ZnO exhibit dual mode luminescence characteristics. They are excitable by UV as well as IR light and the emission spectra also differ.

#### 4.6 Chromaticity of the lanthanide doped dual excitation ZnO

The chromaticity co-ordinates of both DC and UC emission for undoped and lanthanide doped ZnO samples have been calculated from their respective emission spectra according to



and microcrystals with varied morphology. Whereas undoped ZnO synthesized in identical conditions yield cyan fluorescence, Er<sup>3+</sup>/Ho<sup>3+</sup> doping changes the fluorescence colour to different hues of red under band edge (377 nm) UV excitation. RE doped ZnO samples exhibit UC luminescence with colour ranging from green to orange red due to different emission ratio of green and red depending upon the light emitting ion Er<sup>3+</sup>/Ho<sup>3+</sup> and sensitizer Yb<sup>3+</sup>. The results conclusively show that ZnO can function as a phosphor in dual excitation mode of both down and up conversion at the same time and the emission can be tuned widely in the visible range through trivalent lanthanide doping. Such ZnO samples with dual excitation and tunable dual emission have immense potential in light emitting devices and solar cell applications.

## Acknowledgements

This present work was supported by the TAPSUN project under CSIR Solar Mission program of India.

## References

- 1 E. Downing, L. Hesselik, J. Raltson and R. Macfarlane, *Science*, 1996, **273**, 1185.
- 2 F. Van de Rijke, H. Zijlmans, S. Li, T. Vail, A. K. Raap, R. S. Niedbala and H. J. Tanke, *Nat. Biotechnol.*, 2001, **19**, 273.
- 3 G. S. Yi, H. C. Lu, S. Y. Zhao, G. Yue, W. J. Yang, D. P. Chen and L. H. Guo, *Nano Lett.*, 2004, **42**, 191.
- 4 L. Wang, R. X. Yan, Z. Y. Hao, L. Wang, J. H. Zeng, J. Bao, X. Wang, Q. Peng and Y. D. Li, *Angew. Chem., Int. Ed.*, 2005, **44**, 6054.
- 5 B. Y. Oh, M. C. Jeong, T. H. Moon, W. Lee, J. M. Myoung, J. Y. Hwang and D. S. Seo, *J. Appl. Phys.*, 2006, **99**, 124505.
- 6 A. Gupta and A. D. Compaan, *Appl. Phys. Lett.*, 2004, **85**, 684.
- 7 Z. L. Wang, *Annu. Rev. Phys. Chem.*, 2004, **55**, 159.
- 8 C. S. Rout, A. R. Raju, A. Govindaraj and C. N. R. Rao, *Solid State Commun.*, 2006, **138**, 136.
- 9 Z. L. Wang, C. K. Lin, X. M. Liu, Y. Luo, Z. W. Quan, H. P. Xiang and L. Lin, *J. Phys. Chem. B*, 2006, **110**, 9469.
- 10 G. Seisenberger, M. U. Ried, T. Endress, H. Buning, M. Hallek and C. Brauchle, *Science*, 2001, **294**, 1929.
- 11 J. M. Daewas, P. Dekker, P. Burns and J. A. Piper, *Opt. Rev.*, 2005, **12**, 101.
- 12 G. S. Yi, B. Q. Sun, F. Z. Yang, D. P. Chen, Y. X. Zhou and J. Cheng, *Chem. Mater.*, 2002, **14**, 2910.
- 13 S. Heer, K. Kompe, H. U. Gudel and M. Haase, *Adv. Mater.*, 2004, **16**, 2102.
- 14 M. U. Staudt, S. R. Hastings-Simon, M. Nilsson, M. Afzelius, V. Scarani, R. Ricken, H. Suche, W. Sohler, W. Tittel and N. Gisin, *Phys. Rev. Lett.*, 2007, **98**, 113601.
- 15 H. Desirena, E. De la Rosa, A. L. Diaz-Torres and A. G. Kumar, *Opt. Commun.*, 2006, **281**, 560.
- 16 J. S. John, J. I. Coffey, Y. Chen and R. F. Pinnizzotto, *Appl. Phys. Lett.*, 2000, **77**, 1635.
- 17 R. Deng, X. T. Zhang, E. Zhang, Y. Liang, Z. Liu, H. Xu, *et al.*, *J. Phys. Chem. C*, 2007, **111**, 13013.
- 18 Y. Liu, Q. Yang and C. Xu, *J. Appl. Phys.*, 2008, **104**, 064701.
- 19 X. Wang, X. Kong, G. Shan, Y. Yu, Y. Sun, L. Feng, K. Chao, S. Lu and Y. Li, *J. Phys. Chem. B*, 2004, **108**, 18408–18413.
- 20 L. Wang, X. Wang, Z. Li, P. Liu, F. Liu, F. Song, S. Ge, B. Liu, Y. Shi and R. Zhang, *J. Phys. D: Appl. Phys.*, 2011, **44**, 155404.
- 21 Y. Bai, Y. Wang, K. Yang, X. Zhang, Y. Song and C. H. Wang, *Opt. Commun.*, 2008, **281**, 5448–5452.
- 22 X. Yun, S. Liang, Z. Sun, Y. Duan, Y. Qin, L. Duan, H. Xia, P. Zhao and D. Li, *Opt. Commun.*, 2014, **313**, 90–93.
- 23 K. Jayanthi, S. Chawla, K. N. Sood, M. Chhibara and S. Singh, *Appl. Surf. Sci.*, 2009, **255**, 5869–5875.
- 24 K. Jayanthi, S. Chawla, A. Joshi, Z. H. Khan and R. K. Kotnala, *J. Phys. Chem. C*, 2010, **114**, 18429–18434.
- 25 B. Lin, Z. Fu and Y. Jia, *Appl. Phys. Lett.*, 2001, **79**, 945.
- 26 X. Bai, H. Song, G. Pan, Y. Lei, T. Wang, X. Ren, S. Lu, B. Dong, Q. Dai and L. Fan, *J. Phys. Chem. C*, 2007, **111**, 13611–13617.
- 27 L. A. D. Torres, E. D. L. R. Cruz, P. Salas and C. A. Chavez, *J. Phys. D: Appl. Phys.*, 2004, **37**, 2489–2495.
- 28 J.-C. Boyer, L. A. Cuccia and J. A. Capobianco, *Nano Lett.*, 2007, **7**, 847–852.
- 29 D. Matsuura, *Appl. Phys. Lett.*, 2002, **82**, 4526.
- 30 G. Y. Chen, Y. G. Zhang, G. Somestalean, Z. G. Zhang, Q. Sun and F. P. Wang, *Appl. Phys. Lett.*, 2006, **89**, 163105.
- 31 F. Vetrone, J. C. Boyer, J. A. Capobianco, A. Speghini and M. Bettinelli, *Appl. Phys. Lett.*, 1752, **2002**, 80.
- 32 X. X. Luo and W. H. Cao, *Mater. Lett.*, 2007, **61**, 3696–3700.
- 33 Kelmer, *Luminescent Screens: Photometry and Colorimetry 118*, Iliffe, London, 1969.